

# Configuration Dynamics of a Flexible Polymer Chain in a Bath of Chiral Active Particles

Xinshuang Liu, Huijun Jiang,\* and Zhonghuai Hou†

*Department of Chemical Physics & Hefei National Laboratory for Physical Sciences at Microscales,  
University of Science and Technology of China, Hefei, Anhui 230026, China*

(Dated: August 27, 2019)

We investigate configuration dynamics of a flexible polymer chain in a bath of active particles with dynamic chirality, i.e., particles rotate with a deterministic angular velocity  $\omega$  besides self-propulsion, by Langevin dynamics simulations in two dimensional space. Particular attentions are paid to how the gyration radius  $R_g$  changes with the propulsion velocity  $v_0$ , angular velocity  $\omega$  and chain length. We find that in a chiral bath with a typical nonzero  $\omega$ , the chain first collapses into a small compact cluster and swells again with increasing  $v_0$ , in quite contrast to the case for a normal achiral bath ( $\omega = 0$ ) wherein a flexible chain swells with increasing  $v_0$ . More interestingly, the polymer can even form a closed ring if the chain length is large enough, which may oscillate with the cluster if  $v_0$  is large. Consequently, the gyration radius  $R_g$  shows nontrivial non-monotonic dependences on  $v_0$ , i.e., it undergoes a minimum for relatively short chains, and two minima with a maximum in between for longer chains. Our analysis shows that such interesting phenomena are mainly due to the competition between two roles played by the chiral active bath: while the persistence motion due to particle activity tends to stretch the chain, the circular motion of the particle may lead to an effective osmotic pressure that tends to collapse the chain. In addition, the size of the circular motion  $R_0 = v_0/\omega$  shows an important role in that the compact clusters and closed-rings are both observed at nearly the same values of  $R_0$  for different  $\omega$ .

## I. INTRODUCTION

As the volume fraction of large macromolecules and other inclusions in cell interior can be as large as 50% [1], crowded environment has been reported to be a key factor in many life processes including chromosome organization [2], polymer translocation through nanopore [3, 4], gene expression [5], and so on. Specifically, configuration change of polymers in crowded environments has gained extensive research attentions in last decades [6–25], due to its close relevance to many crucial biological processes [21–25]. For instance, compared to the non-crowded environment, a polymer chain has a tendency to collapse into a compact structure and increase looping probability in a crowded environment [14–22]. Such a collapse was found to be dependent on the size of the crowder, since smaller crowders exert a higher osmotic pressure onto the polymer and make the polymer chain collapse into a more compact structure as compared to the bigger ones [21]. In addition, polymer rigidity also played an important role on the looping characteristics of a linear polymer chain in crowded environment [14], to list just a few.

It is noted that, crowders in many similar studies are all assumed to be passive, i.e., the crowders themselves will finally relax to an equilibrium state determined by temperature and their interaction potentials. Nevertheless, the crowders may also be active ones which spontaneously take up energy from the environment and con-

vert into their directed motions. Actually, explosive new non-equilibrium phenomena in active systems have been reported in recent years [26–42], both experimentally and theoretically. In particular, dynamics of polymer in active crowded environments also shows many nontrivial phenomena [42–48]. Kaiser and Löwen found that the polymer extension follows a two-dimensional Flory scaling for very long chains, while the active crowders can stiffen and expand the chain in a nonuniversal way for short chains [43]. Harder et al. revealed that, the polymer collapses into a metastable hairpin for a moderate activity of the crowders, and reexpands eventually as the activity increases to be large enough for a rigid polymer chain [44]. Shin et al. investigated the influence of active crowders on polymer looping, and found that increasing the activity yields a higher effective temperature and thus facilitates the looping kinetics of the polymer chain [45].

Besides of the activity, the motion of crowders in real active systems may also be dynamically chiral [49–52]. Examples of chiral active particles including sperm cells [49, 50], E.coli swimming in circular trajectories near a surface [51], asymmetric L-shaped microswimmers of circular motion on a substrate [52], etc. Compared to the active crowder without dynamic chirality, the chiral one is affected not only by the active force but also by an extra torque, leading to a circular motion in two dimensional space or a helical motion in three dimensional space. It has been found that the chiral feature of active particles can affect significantly the collective dynamics including transport [53–56], separation [57, 58], sorting [59, 60], and so on. However, to the best of our knowledge, how the dynamic chirality of active crowders would influence the configuration change of a polymer chain has not been studied yet.

\*Electronic address: hjjiang3@ustc.edu.cn

†Electronic address: hzhlj@ustc.edu.cn

Motivated by this, in this paper, we investigate the configuration dynamics of a linear polymer chain immersed in an active bath with dynamic chirality in two dimensional space. Each active particle is self-propelled with a speed  $v_0$  along a direction which changes via random rotational diffusion and besides, a deterministic rotation with angular velocity  $\omega$ . We mainly focus on how the averaged radius  $R_g$  of gyration of the polymer chain depends on the active velocity  $v_0$ , with varying  $\omega$  and chain length  $N$ . Very interestingly, we find that  $R_g$  shows nontrivial non-monotonic dependences on  $v_0$ : it first decreases to a minimum value and then increase again. At the minimum, the chain collapses into a small compact cluster that may rotate in the opposite direction to that of the particles. If the chain is long enough, more interesting behaviors, including a closed ring with some particles rotating inside, and an oscillation between the cluster and the ring, can be observed for moderate levels of particle activity.

The remainder of this paper is organized as follows. In Sec. II, we describe our model and simulation method. In Sec. III, we present our results and discussion followed by conclusions in Sec. IV.

## II. MODEL AND METHOD

We consider a linear polymer chain consisting of  $N$  coarse-grained spring beads with diameter  $\sigma$  immersed in a bath of  $N_c$  chiral active crowder particles in a  $L \times L$  two dimensional space with periodic boundary conditions. The crowders are of the same diameters as the beads. All the non-bonded (excluded volume) interactions among beads and crowders are described by the WCA potential,

$$U_{WCA}(r_{ij}) = \begin{cases} 4\epsilon \left[ \left( \frac{\sigma}{r_{ij}} \right)^{12} - \left( \frac{\sigma}{r_{ij}} \right)^6 + \frac{1}{4} \right] & r_{ij} \leq 2^{1/6}\sigma \\ 0 & r_{ij} > 2^{1/6}\sigma \end{cases}, \quad (1)$$

where  $\epsilon$  denotes the potential strength, and  $r_{ij}$  is the distance between a pair of particles  $i$  and  $j$ , with  $i, j$  running over all the crowders and beads. Besides, the bonded interaction between all neighboring beads in the polymer chain is described by the finite extension nonlinear elastic (FENE) potential,

$$U_{FENE}(r_{ij}) = -\frac{1}{2}\kappa R_0^2 \ln \left[ \left( 1 - \left( \frac{r_{ij}}{R_0} \right)^2 \right) \right] \quad (2)$$

where  $\kappa$  is the elastic coupling constant,  $R_0$  denotes the maximum bond length and  $i, j$  run over the polymer beads.

For the active chiral crowders, the system dynamics obeys the following overdamped Langevin equations

$$d\vec{r}_i/dt = v_0 \vec{u}_i - (1/\gamma) \nabla_i U + \sqrt{2D_0} \xi_i^T(t), \quad (3)$$

$$d\theta_i/dt = \omega + \sqrt{2D_R} \xi_i^R(t), \quad (4)$$

where  $\vec{r}_i$  and  $\theta_i$  are the position and orientation of the  $i$ th crowder, respectively.  $\vec{u}_i \equiv (\cos\theta_i, \sin\theta_i)$  denotes the orientation of the  $i$ th active crowder and  $v_0$  is the active velocity. In particular,  $\omega$  in (2) gives the angular velocity of the particle which is assumed to be the same for all crowders. For  $\omega \neq 0$ , the particle undergoes a circular motion in the absence of the noise term, which determines the chirality of the particle. The model reduces to the usually used ABP (stands for Active Brownian Particles) one for  $\omega = 0$ .

In Eq. (1),  $U$  denotes the total interaction potential in the whole system including all the exclusive-volume and bonded interactions,  $\gamma$  is the friction coefficient of the surrounding medium,  $D_0$  and  $D_R$  are the translational and rotational diffusion coefficients, respectively, which hold the relations of  $\gamma = k_B T / D_0$  and  $D_R = 3D_0 / \sigma^2$  with  $k_B$  the Boltzmann constant and  $T$  the temperature.  $\xi_i^T(t)$  and  $\xi_i^R(t)$  are Gaussian white noises with zero mean and satisfy  $\langle \xi_{i\alpha}^T(t) \xi_{j\beta}^T(s) \rangle = \delta_{ij} \delta_{\alpha\beta} \delta(t-s)$  ( $\alpha, \beta$  denote Cartesian coordinates) and  $\langle \xi_i^R(t) \xi_j^R(s) \rangle = \delta_{ij} \delta(t-s)$ , respectively.

Note that for a polymer bead  $i$ , the dynamics is also described by Eq.(1) except that  $v_0 = 0$ . For simplicity, we use same interaction and diffusion parameters for the polymer beads and the crowder particles.

In simulations,  $\sigma$ ,  $k_B T$ , and  $\tau = \sigma^2 / 10D_0$  are chosen as the dimensionless units for length, energy and time, respectively. Other parameters are chosen as  $L = 50$ ,  $D_0 = 0.1$ ,  $D_R = 0.3$ ,  $\gamma = 10.0$ ,  $\epsilon = 10$ ,  $\kappa = 300$ ,  $R_0 = 1.5$ , and the simulation time step is  $10^{-4}$ . The number of crowders is set to be  $N_c = 318$ , so that its volume fraction is given by  $\phi = 0.1$ . All the data in this paper are averaged over 50 independent simulation runs.

## III. RESULTS AND DISCUSSION

The main purpose of the present work is to investigate how the chiral feature of the crowders would influence the configuration dynamics of the polymer chain. To begin, we consider a chain with fixed length in a chiral active bath with a fixed nonzero angular velocity, but varying the activity velocity  $v_0$ . Fig.1 shows several typical snapshots from our simulations for  $N = 40$  and  $\omega = 1.5\pi$ , with increasing  $v_0$  from a relatively small value  $v_0 = 1$  to a large one  $v_0 = 50$ . When the activity is small as shown in Fig.1(a), the polymer chain keeps a free state (the free state here means that the chain is neither stretched nor collapsed), similar to a polymer chain in a passive environment. With increasing activity to a moderate level as shown for  $v_0 = 15$  in Fig.1(b), interestingly, the polymer chain collapses into a stable compact spiral structure. All the crowder particles move outside this cluster and collide with the cluster. Consequently, the whole cluster rotates in the opposite direction (clockwise) to that of the crowder particles. For further increasing  $v_0$ , for instance

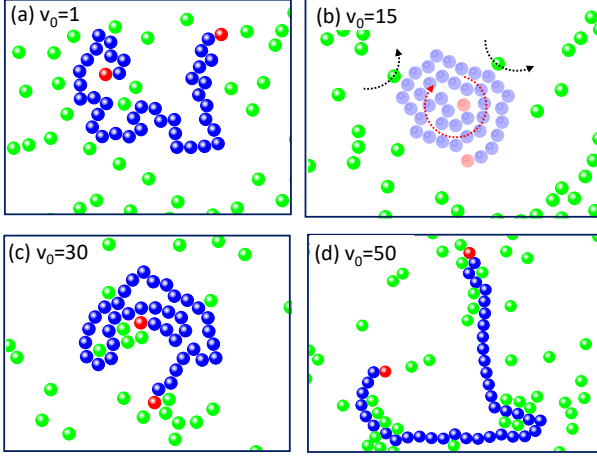


Figure 1: Typical snapshots for the polymer chain (red and blue) in chiral active crowders (green) with  $\omega = 1.5\pi$  and  $N = 40$  for different active velocity  $v_0$ . (a) The polymer chain keeps a free state for  $v_0 = 1$ , (b) and collapses into a stable compact spiral structure rotating oppositely to crowders for  $v_0 = 15$ . (c) The spiral structure is broken for  $v_0 = 30$ , (d) and finally the polymer chain expands for  $v_0 = 50$ .

$v_0 = 30$  in (c), crowders may intrude into the interior of the cluster leading to its breakup and the chain becomes more expanded than the cluster. If the activity is even larger, the crowders would aggregate and adhere to the chain leading to stretching of the chain, as depicted for  $v_0 = 50$  in Fig.1(d).

To quantitatively characterize the phenomena, we have calculated the radius  $R_g$  of gyration of the polymer chain defined as  $R_g = \sqrt{\langle R_g^2 \rangle} = \sqrt{\frac{1}{2N^2} \sum_{i,j} (\mathbf{r}_i - \mathbf{r}_j)^2}$ . In

Fig.2(a),  $R_g$  is presented as a function of the velocity  $v_0$  (dash-dotted line), wherein a clearcut non-monotonic behavior is observed:  $R_g$  first decreases from  $R_g^0$ , the gyration of radius in the absence of activity ( $v_0 = 0$ ), to a minimum value at  $v_0 \sim 15$  corresponding to the compact spiral cluster shown in Fig.1(b) and then increases with increasing activity. Finally,  $R_g$  becomes larger than  $R_g^0$  indicating that the polymer chain swells for large enough activity. For comparison, the result for achiral crowders, i.e.  $\omega = 0$ , is also shown (dashed line). Clearly, the behavior is quite distinct from that for chiral crowders with  $\omega = 1.5\pi$ :  $R_g$  increases monotonically with  $v_0$ , in consistent with the results reported in Ref.[43] where it was shown that activity always leads to swelling of flexible polymer chains. Therefore, chiral active crowders have very nontrivial effects to the configuration dynamics of the polymer chain, in particular, they lead to collapse of the chain to a compact cluster before swelling.

To get more information about the configuration at different activity level, we have also measured the probability distribution function  $P(R_g)$ , as depicted in Fig.2(b). All the distributions are unimodal, i.e., the gyration radius peaks around a most probable value. With increas-

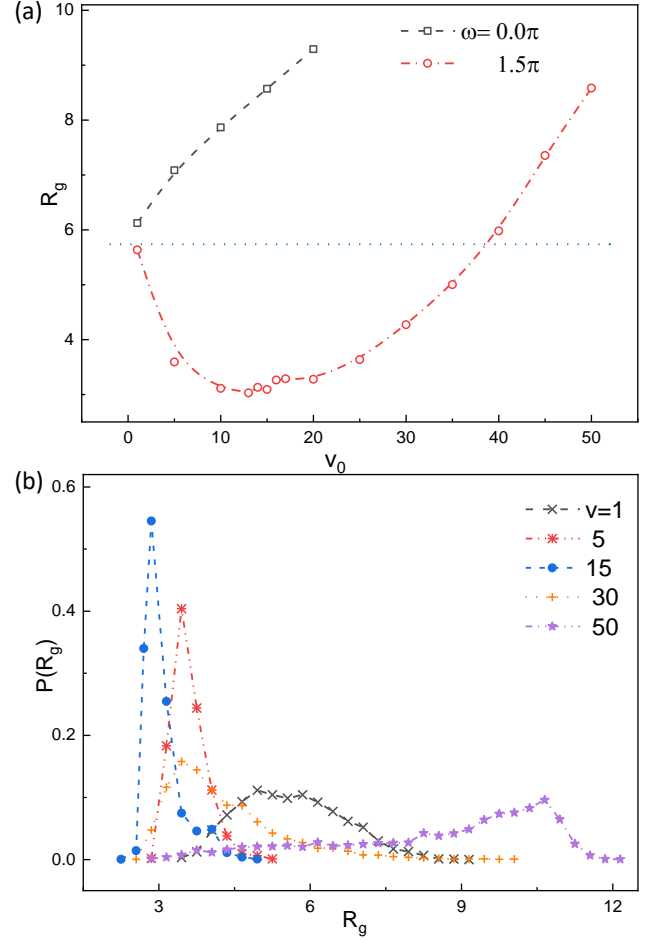


Figure 2: (a) The radius  $R_g$  of gyration of the polymer chain with length  $N = 40$  as a function of active velocity  $v_0$  for an achiral active bath and a chiral one. The horizontal dotted line is  $R_g^0$ . (b) Probability distribution  $P(R_g)$  of the gyration radius  $R_g$  for the polymer chain with  $N = 40$  with different active velocity  $v_0$  and fixed angular velocity  $\omega = 1.5\pi$ .

ing activity, the peak first shifts to small values of  $R_g$  and then to large values if activity is large, corresponding to the non-monotonic dependence of  $R_g$  with  $v_0$  shown in Fig.2(a). In addition, one can see that the peak width also shows non-monotonic variations with increasing  $v_0$ . In particular, the distribution becomes sharply peaked for  $v_0 \sim 15$ , wherein the polymer collapses into a compact cluster. Such small fluctuations of  $R_g$  indicates that this spiral cluster is quite stable during the time evolution.

Without doubt, the activity-induced collapse behavior observed above is due to the chiral feature of the active crowders. As already mentioned above, the polymer chain would only swell with the increment of crowder activity  $v_0$  in the absence of chirality ( $\omega = 0$ ). An achiral active particle, such as the usual active Brownian particle, would undergo a persistent motion along the original orientation with a persistence length given

by  $v_0\tau_p = v_0(2D_r)^{-1}$  before changing its direction randomly according to random rotation. Therefore, such active particles tend to adhere and aggregate onto the polymer chain, thus exert a ‘pulling’ force to the polymer beads resulting in a net expanding effect on the chain length. A particle will stay aside the polymer chain until its direction changes to an escape cone and not hindered by peripheral particles. With increasing activity, the persistence length increases and the force each active particle exerts onto the chain also increases, leading to more expanded configuration.

However, such a scenario is not totally true for chiral active particles. Clearly, an isolated chiral active particle would undergo a deterministic circular motion with a radius given by  $R_0 = v_0/\omega$  if noise is absent (for  $\omega > 0$ , the particle rotates counter-clockwisely). Once it collides with the polymer chain, its direction can change due to this circular motion within a time scale given by  $\omega^{-1}$ , unlike the case for achiral particle for which the direction can only change via random rotation with a characteristic time scale given by  $\tau_p$ . Such a deterministic circular motion of chiral active particles would prevent them from adhering to the polymer chain. In addition, the circular motion of size  $R_0$  also makes it hard for the particle to stay in the ‘interior’ part of the chain (locally concave), which will lead to a difference of pressure between the ‘interior’ and ‘exterior’ parts of the chain, thus causing the collapse behavior.

To get more details of the collapse process, we have investigated how  $R_g$  change with time for  $v_0 = 15$  (corresponding to the compact structure shown in Fig.1b) as presented in Fig.3. Correspondingly, some typical snapshots are also shown. One can see that  $R_g$  reduces monotonically (with fluctuations) to the steady state value in a relatively short period of time. In the early stage, the chain is in an elongated state (the first snapshot). Shortly, the chain is rolled up from both ends forming two small connected compact clusters, wherein no crowders exists in the interior parts. Note that the two ends roll up in the same clockwise direction (note here the angular velocity of the crowders  $\omega > 0$ , i.e., the circular motion is anticlockwise). These two clusters grow up in size with time until they collide with each other as shown by the third snapshot. By chance, one cluster will finally enslave the other and the two clusters combine into one, rotating clockwise with one end in and the other end out, as shown by the last snapshot in Fig.3 which is the same as in Fig.1(b).

The above analysis shows that circular motion is the very reason for polymer collapse. In addition, the size  $R_0$  seems to play an important role. If  $R_0$  is too small, which is the case for small  $v_0$ , the effect of chirality is not strong and the crowder particle acts as a normal achiral one, such that they can still stay in the interior part of the chain and the pressure difference mentioned in the last paragraph would be small. In this situation, the collapse effect would also be small. With the increasing of activity,  $R_0$  will also increase and fewer particles can

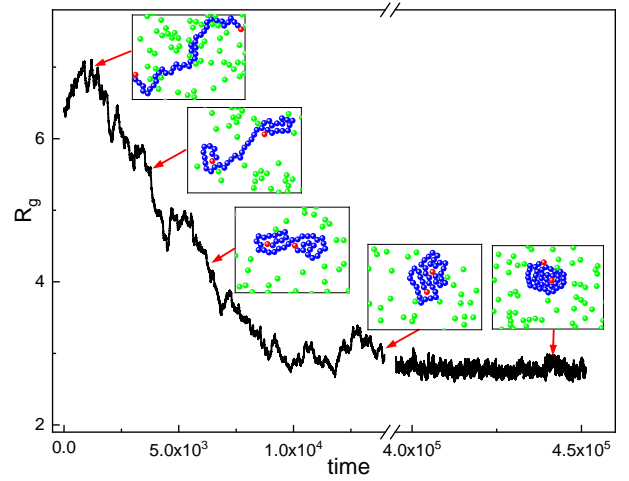


Figure 3: Time dependence of the gyration radius  $R_g$  for a polymer chain  $N = 40$  at  $v_0 = 15$  and  $\omega = 1.5\pi$ .

stay ‘inside’ the chain, leading to more strong collapse effect and decreasing  $R_g$ . Of course, the most collapsed configuration of the chain that could be reached is the compact one as shown in Fig.1(b).

Note however, increasing particle activity also has another effect, i.e., the increase of persistence length of the active motion, which is the reason for polymer stretching as already discussed above. If the activity is too large,  $R_0$  would be even larger than the characteristic length of the chain, and the chain would not ‘feel’ the circular motion of the particle. Once the particle collide and adhere to the chain, it will undergo persistence motion along the chain, just like an achiral active particle. Therefore, the polymer chain would be elongated again with increasing activity.

To summarize so far, we understand that dual effects exist for chiral active crowders on the configuration dynamics of the polymer chain. On one hand, the circular motion leads to an effect like osmotic pressure that results in polymer collapse. On the other hand, the persistence motion would cause stretching of the chain thus leading to swelling. With increasing activity level  $v_0$ , such two effects will compete with each other. Firstly, the collapse effect dominates, but finally the swelling effect will take the dominant role. Consequently,  $R_g$  shows a non-monotonic dependence on  $v_0$ , namely, it first decreases to a minimum value and then increases again to a value that is larger than  $R_g^0$ .

All above results are obtained for a fixed angular velocity  $\omega = 1.5\pi$ . One may thus wonder how the findings depend on  $\omega$ . The results are presented in Fig.4(a), where the dependences of  $R_g$  as functions of  $v_0$  are shown for a few different values of  $\omega$  ranging from a very small value  $\omega = 0.125\pi$  to a large one  $3.0\pi$ . One can see that for a very small  $\omega$  (say  $0.125\pi$ ), the polymer already collapses for a small  $v_0$  ( $R_g < R_g^0$ ), but  $R_g$  increases with  $v_0$  (the minimum locates at a very small  $v_0$  out of the shown range). With increasing  $\omega$ , the non-monotonic depen-

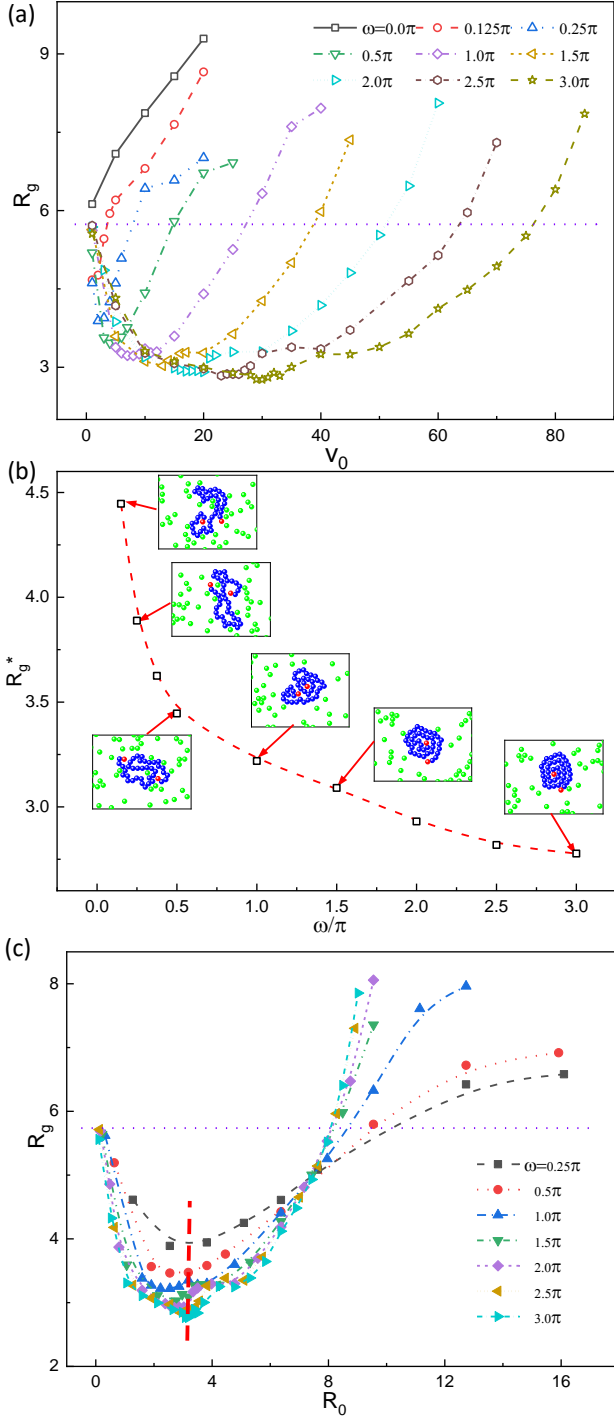


Figure 4: (a) The radius  $R_g$  of gyration of the polymer chain with length  $N = 40$  as a function of active velocity  $v_0$  for different angular velocity  $\omega$ . (b) Dependence of  $R_g^*$  on angular velocity  $\omega$ . (c) The radius  $R_g$  of gyration of the polymer chain as a function of the size of the circular motion  $R_0$  for different angular velocity  $\omega$ . The horizontal dotted line in (a) and (c) is  $R_g^0$ .

dence of  $R_g$  with  $v_0$  becomes apparent and the location of  $v_0$  for the minimum shifts to larger values. Meanwhile, the minimum  $R_g^*$  decreases until it saturates to the smallest value corresponding to a compact cluster, as demonstrated in Fig.4(b). Also shown in (b) are typical configurations of the chain with the minimum  $R_g$ . We note here that for small  $\omega$ , the most collapsed structure of the chain is not the spiral cluster as that for large values of  $\omega$ . If  $\omega$  is very small such that characteristic time scale for deterministic rotation is larger than the persistence time  $\tau_p$  of the active motion, the particle may attach to the chain for a time about  $\tau_p$  before it rotates out. Consequently, some particles can stay ‘inside’ the chain as shown in the snapshots in (b) and  $R_g$  is not that small.

The data in Fig.4(a) show that the minimum shifts to larger value of  $v_0$  with increasing  $\omega$ . As already mentioned above, the size of the circular motion  $R_0 = v_0/\omega$  plays an important role to the collapse behavior of the chain. It suggests us to see how  $R_g$  changes with this size parameter  $R_0$ . In Fig.4(c),  $R_g$  is drawn as a function of  $R_0$  instead of  $v_0$  for different values of  $\omega$ . Very interestingly, the locations of minimum are nearly the same (see the vertical dashed line), i.e., the chain becomes most collapsed at the same value of  $R_0$ . Therefore, it is the effective size  $R_0$  that mainly determines the collapse behavior of the chain. It should be instructive to perform some theoretical analysis about how  $R_g^*$  depends on  $R_0$ , but it seems to be quite hard and beyond the scope of current study.

In Fig.4(b),  $R_g^*$  reaches a constant value for large values of  $\omega$ , corresponding to the close-packed cluster structure of the chain. Clearly, this constant value of  $R_g^*$  is decided by the chain length  $N$ . One may then ask how the above observations depend on the chain length. At first thought, no qualitative difference would be expected for different  $N$ , however, this is not the case. In Fig.5(a), the dependence of  $R_g$  on  $v_0$  is shown for  $\omega = 1.5\pi$ , with same parameters as in Fig.(2a), but now for  $N = 60$ . Again, one can see that  $R_g$  decreases with  $v_0$  increasing from  $v_0 = 1$ , reaches a minimum at  $v_0 \simeq 15$  and then increases again, similar to that observed for  $N = 40$ . But surprisingly,  $R_g$  shows quite nontrivial non-monotonic behaviors in the range of moderate values of  $v_0$ , namely, it undergoes a maximum at  $v_0 \simeq 22$  and another minimum at  $v_0 \simeq 30$  before finally increasing monotonically, which was not observed at all for  $N = 40$ .

To get more details, we have calculated the distribution of  $R_g$  at those three extreme values of  $v_0$  and drawn the typical snapshots of the chain, as presented in Fig.5(b). At the first minimum  $v_0 \simeq 15$ , the distribution is unimodal similar to that for  $N = 40$ , and the corresponding configuration is also a compact spiral cluster as given by the inset snapshot. For  $v_0 = 22.5$ , which is the location for the maximum of  $R_g$ , the distribution is also unimodal and sharp-peaked with an average  $R_g$  larger than that for  $v_0 = 15$ . Interestingly, now the typical configuration of the chain is a closed-ring, which is hollow with some crowder particles moving inside. The ring rotates in the

same direction (anticlockwisely) as the crowders, which is quite different from the cluster observed at  $v_0 = 15$ , that rotates in the opposite direction as the crowders. For  $v_0 = 30$  where the average  $R_g$  is at a local minimum, however, the distribution of  $R_g$  is bimodal with two peaks, one at  $R_g \simeq 3.5$  that is close to the peak position for  $v_0 = 15$ , and the other at  $R_g \simeq 5.5$  close to the peak position for  $v_0 = 22.5$ . Correspondingly, typical snapshots for the two peaks are shown in the same figure, wherein the first peak is related to the cluster structure and the second one to the ring-structure. Watching the dynamic process, we find that the polymer chain actually oscillates between these two structures. In Fig.5(c), we have drawn the time dependence of  $R_g$  for  $v_0 = 30$ , where one can observe quite obvious oscillation behavior. We note here that similar oscillation behaviors are observed for a quite range of  $v_0$  to the right side of the maximum.

Here we would like to point out that the rotation directions of the cluster (for  $v_0 = 15$ ) and the ring (for  $v_0 = 22.5$ ) observed here are consistent with those observations in Ref.[61] and Ref. [62]. In Ref.[61], the authors studied the phase separation of chiral active crowders, finding that the passive cluster rotates in the opposite direction to that of the chiral active particles. There the authors argued that the passive cluster with non-smooth boundary formed a ‘gear’, which was the reason for opposite rotating behavior. The same reasoning also works for the spiral cluster formed by the polymer chain here. While in Ref.[62], Chen et al. studied the behavior of a closed ring (note the ends are connected there) with some chiral active particles inside. They found that the ring rotated continuously in the same direction as the active particles for a proper level of activity, which is similar to what we observed for  $v_0 = 22.5$  here. Note that the ring-configuration observed in our present study is dynamically formed during the process, with active particles dynamically going in and out in a stationary way.

The results observed for  $N = 60$  further demonstrate that nontrivial roles played by the chiral crowders on the chain dynamics. The formation of the compact cluster structure at the first minimum can be understood in the similar way as that for  $N = 40$ , which is due to the circular motion of the chiral particle. The ring configuration observed at a moderate value of  $v_0 = 22.5$ , which was not observed for  $N = 40$ , is also closely related to the circular motion of the chiral crowders. For this ring to be formed, the chain length must be large enough to support the circular motion of crowders inside, thus it can not be observed if the chain is too short. The crowders moving inside the ring collide with the polymer beads and expand the ring, making the ring rotates in the same direction as the circular motion as mentioned above. The crowders outside the ring, however, tend to collapse the ring and rotate the ring in the opposite direction. If the activity level is small, the circular motion size  $R_0$  is not large enough to sustain the ring from inside. If activity is too large, on the other hand, the pressure outside the

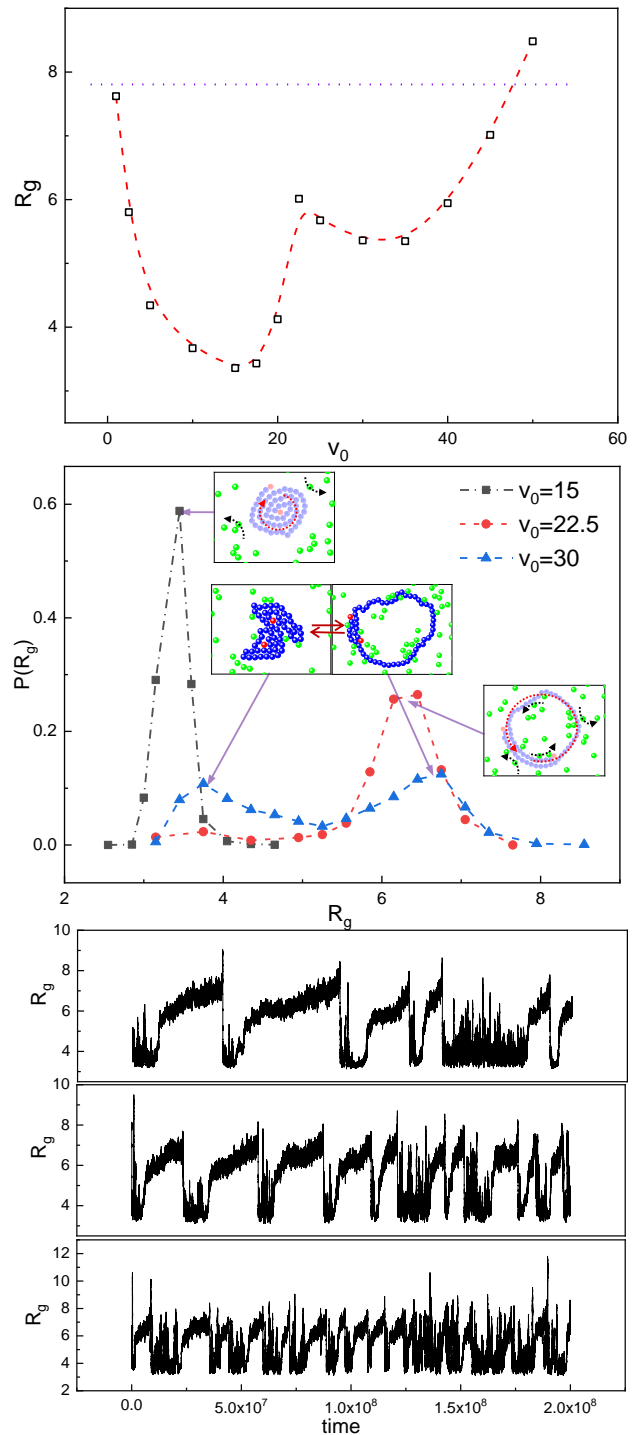


Figure 5: (a) The radius  $R_g$  of gyration of the polymer chain with length  $N = 60$  as a function of active velocity  $v_0$ . The horizontal dotted line is  $R_g^0$ . (b) Probability distribution  $P(R_g)$  of the gyration radius  $R_g$  for various active velocity  $v_0$ . (c) Time dependence of the gyration radius  $R_g$  for a polymer chain  $N = 60$  for several active velocity  $v_0$ . The angular velocity is fixed as  $\omega = 1.5\pi$ .



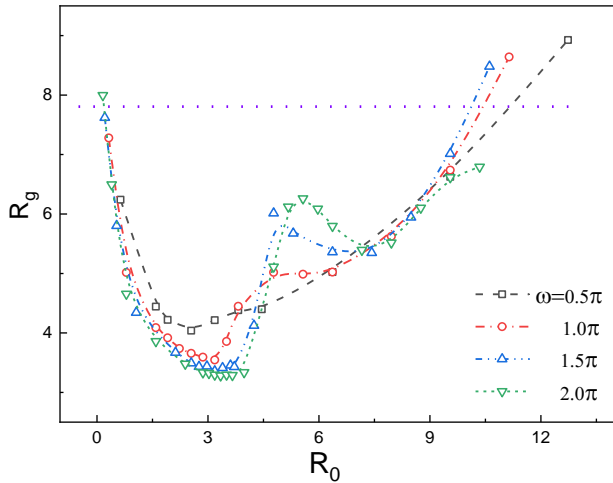


Figure 6: The radius  $R_g$  of gyration of the polymer chain as a function of the size of the circular motion  $R_0$  for different angular velocity  $\omega$ .

ring would dominate (since the particles inside the ring is limited) causing instability of the ring. The competition between the different effects inside/outside the ring thus leads to the non-monotonic as well as oscillating behaviors observed for the moderate levels of  $v_0$ . If  $v_0$  is very large, the stretching effect would dominate finally resulting in monotonic increasing of  $R_g$  again. We also note here that these behaviors observed for  $N = 60$  are also present for longer chains except that the locations of  $v_0$  for the minimum or maximum are different. Therefore, the results reported here for  $N = 40$  and  $60$  already outline the main dynamics of a flexible chain in chiral active crowders.

Finally, we have also investigated the results for  $N = 60$  for different values of  $\omega$ . As in Fig.4(c), we draw  $R_g$  as a function of  $R_0 = v_0/\omega$ , as shown in Fig.6. A few remarks can be made regarding the results. Firstly, the maximum of  $R_g$  is not apparently observed for small  $\omega$  (see for instance  $\omega = 0.5\pi$  and  $1.0\pi$ ), indicating that the ring structure can not be stably formed. Secondly, we also find that the positions of  $R_0$  for the first minimum (for cluster structure) are still nearly the same similar to the case for  $N = 40$ . More interestingly, once the maximum (for ring structure) exists, it also takes place at nearly the same value of  $R_0$ . Finally, the oscillation behavior is robust if  $\omega$  is not small, and the location of the second minimum also takes place at nearly same  $R_0$ . All these findings demonstrate the key role of the circular motion, which is the very characteristics of chiral active particles, and underline a type of size effect which deserves more study in future works.

#### IV. CONCLUSION

In conclusion, we have used Langevin dynamics simulation to investigate the configuration dynamics of a flex-

ible linear polymer chain in a bath of active crowder particles with dynamic chirality, i.e., each particle undergoes self-propelled active motion with velocity  $v_0$  along an orientation which changes via random rotational diffusion besides a deterministic circular motion with angular velocity  $\omega$ . Different from the results for chain dynamics in a purely achiral active bath where the chain swells monotonically with increasing  $v_0$ , it was found that the average radius of gyration  $R_g$  of the chain shows quite interesting non-monotonic dependences on  $v_0$  if  $\omega$  is observably nonzero. In particular, the chain collapses for small values of  $v_0$  while it swells if  $v_0$  is large enough, such that  $R_g$  reaches a minimum value  $R_g^*$  at a moderate  $v_0^*$ . Interestingly, the chain is suppressed to a rotating compact cluster at this minimum if  $\omega$  is not small, of which the rotation direction is opposite to the crowder particles. In addition, we found that the size  $R_0 = v_0/\omega$  of the circular motion plays a subtle role, in that the minima for different values of  $\omega$  take places at nearly the same value of  $R_0$ . Our analysis revealed that chiral active bath can result in two-fold effects on polymer configuration dynamics: one of which is that the persistence motion of the active particles leads to stretching of the polymer chain and makes the chain swell, and the other is that the circular motion of the particle leads to an osmotic-pressure-like effect that results in polymer collapse. It is the competition between these two effects that results in the nontrivial dependence of chain dynamics on particle activity. If the chain is long enough, even more interesting phenomena can be observed if  $v_0$  is larger than  $v_0^*$ : the chain can form a hollow closed-ring rotating with the same direction as that of the crowders, also taking place at nearly the same values of  $R_0$ , and the ring may lose stability if  $v_0$  is even larger, leading to interesting oscillating behavior between the closed-ring and the compact cluster. As a consequence, for relatively long chains,  $R_g$  undergoes two minima as  $v_0$  increases, with a maximum between them. Our results clearly demonstrate that chain dynamics in a chiral active bath is considerably different from that in a normal achiral one and highlight the nontrivial roles played by the particle chirality. Our work may shed new lights on the study of active particles systems since chiral active baths are of ubiquitous importance in real biological active systems.

#### Acknowledgments

This work is supported by MOST(2016YFA0400904, 2018YFA0208702), by NSFC (21973085, 21833007, 21790350, 21673212, 21521001, 21473165), by the Fundamental Research Funds for the Central Universities (WK2340000074), and Anhui Initiative in Quantum Information Technologies (AHY090200).

- 
- [1] A. B. Fulton, *Cell* **30**, 345 (1982).
  - [2] J. Pelletier, K. Halvorsen, B.-Y. Ha, R. Paparcone, S. J. Sandler, C. L. Woldringh, W. P. Wong, and S. Jun, *Proc. Natl. Acad. Sci. U.S.A.* **109**, E2649 (2012).
  - [3] A. Gopinathan and Y. W. Kim, *Phys. Rev. Lett.* **99**, 228106 (2007).
  - [4] V. V. Palyulin, T. Ala-Nissila, and R. Metzler, *Soft matter* **10**, 9016 (2014).
  - [5] C. Tan, S. Saurabh, M. P. Bruchez, R. Schwartz, and P. LeDuc, *Nat. Nanotechnol.* **8**, 602 (2013).
  - [6] E. J. Foster, E. B. Berda, and E. Meijer, *J. Am. Chem. Soc.* **131**, 6964 (2009).
  - [7] K. Haydukivska and V. Blavatska, *J. Chem. Phys.* **141**, 094906 (2014).
  - [8] D. Hu, J. Yu, K. Wong, B. Bagchi, P. J. Rossky, and P. F. Barbara, *Nature* **405**, 1030 (2000).
  - [9] J. Kim, C. Jeon, H. Jeong, Y. Jung, and B.-Y. Ha, *Soft Matter* **11**, 1877 (2015).
  - [10] S. Majumder, J. Zierenberg, and W. Janke, *Soft matter* **13**, 1276 (2017).
  - [11] J. Shin, A. G. Cherstvy, and R. Metzler, *Soft matter* **11**, 472 (2015).
  - [12] Y. Bian, X. Cao, P. Li, and N. Zhao, *Soft matter* **14**, 8060 (2018).
  - [13] N. M. Toan, D. Marenduzzo, P. R. Cook, and C. Micheletti, *Phys. Rev. Lett.* **97**, 178302 (2006).
  - [14] J. Shin, A. G. Cherstvy, and R. Metzler, *ACS Macro Letters* **4**, 202 (2015).
  - [15] C. Jeon, Y. Jung, and B.-Y. Ha, *Soft matter* **12**, 9436 (2016).
  - [16] O. Stiehl, K. Weidner-Hertrampf, and M. Weiss, *New J. Phys.* **15**, 113010 (2013).
  - [17] M. Eilers and G. Schatz, *Cell* **52**, 481 (1988).
  - [18] J. S. Kim, V. Backman, and I. Szleifer, *Phys. Rev. Lett.* **106**, 168102 (2011).
  - [19] A. Chen and N. Zhao, *Phys. Chem. Chem. Phys.* (2019).
  - [20] J. Wang, Y. Bian, X. Cao, and N. Zhao, *AIP Adv.* **7**, 115120 (2017).
  - [21] H. Kang, P. A. Pincus, C. Hyeon, and D. Thirumalai, *Phys. Rev. Lett.* **114**, 068303 (2015).
  - [22] S. Prakash and A. Matouschek, *Trends Biochem. Sci.* **29**, 593 (2004).
  - [23] D. Rodriguez-Larrea and H. Bayley, *Nat. Nanotechnol.* **8**, 288 (2013).
  - [24] D. Balchin, M. Hayer-Hartl, and F. U. Hartl, *Science* **353**, aac4354 (2016).
  - [25] G.-W. Li, O. G. Berg, and J. Elf, *Nat. Phys.* **5**, 294 (2009).
  - [26] A. Czirók and T. Vicsek, *Physica. A* **281**, 17 (2000).
  - [27] D. Woolley, *Reproduction* **126**, 259 (2003).
  - [28] A. Sokolov, I. S. Aranson, J. O. Kessler, and R. E. Goldstein, *Phys. Rev. Lett.* **98**, 158102 (2007).
  - [29] T. Vicsek and A. Zafeiris, *Phys. Rep.* **517**, 71 (2012).
  - [30] Y. Fily and M. C. Marchetti, *Phys. Rev. Lett.* **108**, 235702 (2012).
  - [31] J. Schwarz-Linek, C. Valeriani, A. Cacciuto, M. Cates, D. Marenduzzo, A. Morozov, and W. Poon, *Proc. Natl. Acad. Sci. U.S.A.* **109**, 4052 (2012).
  - [32] R. Wittkowski, A. Tiribocchi, J. Stenhammar, R. J. Allen, D. Marenduzzo, and M. E. Cates, *Nat. Commun.* **5**, 4351 (2014).
  - [33] J. Stenhammar, R. Wittkowski, D. Marenduzzo, and M. E. Cates, *Phys. Rev. Lett.* **114**, 018301 (2015).
  - [34] J. A. Cohen and R. Golestanian, *Phys. Rev. Lett.* **112**, 068302 (2014).
  - [35] J. Dunkel, S. Heidenreich, K. Drescher, H. H. Wensink, M. Bär, and R. E. Goldstein, *Phys. Rev. Lett.* **110**, 228102 (2013).
  - [36] H. Jiang, H. Ding, M. Pu, and Z. Hou, *Soft matter* **13**, 836 (2017).
  - [37] M. Pu, H. Jiang, and Z. Hou, *Soft matter* **13**, 4112 (2017).
  - [38] H. Ding, H. Jiang, and Z. Hou, *Phys. Rev. E* **95**, 052608 (2017).
  - [39] M. Feng and Z. Hou, *Soft Matter* **13**, 4464 (2017).
  - [40] M.-k. Feng and Z.-h. Hou, *Chin. J. Chem. Phys.* **31**, 584 (2018).
  - [41] Y. Du, H. Jiang, and Z. Hou, *Soft matter* **15**, 2020 (2019).
  - [42] C. Bechinger, R. Di Leonardo, H. Löwen, C. Reichhardt, G. Volpe, and G. Volpe, *Rev. Mod. Phys.* **88**, 045006 (2016).
  - [43] A. Kaiser and H. Löwen, *J. Chem. Phys.* **141**, 044903 (2014).
  - [44] J. Harder, C. Valeriani, and A. Cacciuto, *Phys. Rev. E* **90**, 062312 (2014).
  - [45] J. Shin, A. G. Cherstvy, W. K. Kim, and R. Metzler, *New J. Phys.* **17**, 113008 (2015).
  - [46] M. Pu, H. Jiang, and Z. Hou, *J. Chem. Phys.* **145**, 174902 (2016).
  - [47] N. Nikola, A. P. Solon, Y. Kafri, M. Kardar, J. Tailleur, and R. Voituriez, *Phys. Rev. Lett.* **117**, 098001 (2016).
  - [48] Y.-q. Xia, K. Chen, Y.-q. Ma, et al., *Phys. Chem. Chem. Phys.* **21**, 4487 (2019).
  - [49] G. Corkidi, B. Taboada, C. Wood, A. Guerrero, and A. Darszon, *Biochem. Biophys. Res. Commun.* **373**, 125 (2008).
  - [50] I. H. Riedel, K. Kruse, and J. Howard, *Science* **309**, 300 (2005).
  - [51] E. Lauga, W. R. DiLuzio, G. M. Whitesides, and H. A. Stone, *Biophys. J.* **90**, 400 (2006).
  - [52] F. Kümmel, B. ten Hagen, R. Wittkowski, I. Buttinoni, R. Eichhorn, G. Volpe, H. Löwen, and C. Bechinger, *Phys. Rev. Lett.* **110**, 198302 (2013).
  - [53] J.-j. Liao, X.-q. Huang, and B.-q. Ai, *J. Chem. Phys.* **148**, 094902 (2018).
  - [54] J.-c. Wu, J.-n. Zhou, and B.-q. Ai, *Physica. A* **462**, 864 (2016).
  - [55] B.-q. Ai, *Sci. Rep* **6**, 18740 (2016).
  - [56] C.-t. Hu, Y.-l. Ou, J.-c. Wu, and B.-q. Ai, *J. Stat. Mech.: Theory Exp.* **2016**, 033207 (2016).
  - [57] B.-q. Ai, Y.-f. He, and W.-r. Zhong, *Soft Matter* **11**, 3852 (2015).
  - [58] B. Liebchen and D. Levis, *Phys. Rev. Lett.* **119**, 058002 (2017).
  - [59] M. Mijalkov and G. Volpe, *Soft Matter* **9**, 6376 (2013).
  - [60] Q. Chen and B.-q. Ai, *J. Chem. Phys.* **143**, 09B612-1 (2015).
  - [61] G.-J. Liao and S. H. Klapp, *Soft matter* **14**, 7873 (2018).
  - [62] J. Chen, Y. Hua, Y. Jiang, X. Zhou, and L. Zhang, *Sci. Rep* **7**, 15006 (2017).